Applied Energy 113 (2014) 1575–1585

Contents lists available at ScienceDirect

Applied Energy

journal homepage: www.elsevier.com/locate/apenergy

Lithium iron phosphate based battery – Assessment of the aging parameters and development of cycle life model

Noshin Omar [a,b,*], Mohamed Abdel Monem [a,e], Yousef Firouz [a], Justin Salminen [c], Jelle Smekens [a], Omar Hegazy [a], Hamid Gaulous [d], Grietus Mulder [e], Peter Van den Bossche [b], Thierry Coosemans [a], Joeri Van Mierlo [a]

[a] Vrije Universiteit Brussel, Pleinlaan 2, Brussel 1050, Belgium
[b] Erasmus University College, Nijverheidskaai 170, Brussel 1070, Belgium
[c] VTT Technical Research Centre of Finland, P.O. Box 1000, FI-02044 VTT, Finland
[d] Université de Caen Basse Normandie, Cherbourg-Octeville, France
[e] Vlaamse Instelling voor Technologisch Onderzoek, Unit Energy Technology, Mol, Belgium

HIGHLIGHTS

- Extended life cycle tests.
- Investigation of the battery life cycle at different working conditions.
- Investigation of the impact fast charging on the battery performances.
- Extraction all required relationship for development of a cycle life model.
- Development of a new life cycle model.

ARTICLE INFO

Article history:
Received 8 April 2013
Received in revised form 7 August 2013
Accepted 1 September 2013
Available online 5 October 2013

Keywords:
Lithium-ion batteries
Cycle life tests
Depth of discharge
Discharge current
Working temperature
Fast charging

ABSTRACT

This paper represents the evaluation of ageing parameters in lithium iron phosphate based batteries, through investigating different current rates, working temperatures and depths of discharge. From these analyses, one can derive the impact of the working temperature on the battery performances over its lifetime. At elevated temperature (40 °C), the performances are less compared to at 25 °C. The obtained mathematical expression of the cycle life as function of the operating temperature reveals that the well-known Arrhenius law cannot be applied to derive the battery lifetime from one temperature to another.

Moreover, a number of cycle life tests have been performed to illustrate the long-term capabilities of the proposed battery cells at different discharge constant current rates. The results reveal the harmful impact of high current rates on battery characteristics.

On the other hand, the cycle life test at different depth of discharge levels indicates that the battery is able to perform 3221 cycles (till 80% DoD) compared to 34,957 shallow cycles (till 20% DoD). To investigate the cycle life capabilities of lithium iron phosphate based battery cells during fast charging, cycle life tests have been carried out at different constant charge current rates. The experimental analysis indicates that the cycle life of the battery degrades the more the charge current rate increases. From this analysis, one can conclude that the studied lithium iron based battery cells are not recommended to be charged at high current rates. This phenomenon affects the viability of ultra-fast charging systems.

Finally, a cycle life model has been developed, which is able to predict the battery cycleability accurately.

1. Introduction

Since the beginning of the automobile era, the internal combustion engine (ICE) has been used for vehicular propulsion since the early 1900. In addition, motor vehicles powered by the ICE are significant contributors to air pollutants and greenhouse gases linked to global climate change [1,2]. As the global economy begins to strain under the pressure of rising petroleum prices and environmental concerns, a lot of research work has been spurred the development of various types of clean energy transportation systems such as Hybrid Electric Vehicles (HEVs), Battery Electric Vehicles (BEVs) and Plug-in Hybrid Electric Vehicles (PHEVs) [3–15].

* Corresponding author at: Vrije Universiteit Brussel, Pleinlaan 2, Brussel 1050, Belgium. Tel.: +32 255 915 12.
E-mail address: noshomar@vub.ac.be (N. Omar).

0306-2619/$ - see front matter © 2013 Elsevier Ltd. All rights reserved.
http://dx.doi.org/10.1016/j.apenergy.2013.09.003

However, the energy storage system, with its need for energy for range, power for acceleration, regenerative braking for efficiency and considerable cycle life remains the critical component of the electrically propelled vehicle [15–35].

In HEVs, PHEVs and BEVs, the battery is mostly suffering from various stress factors such as high current rates, deep discharge conditions, low and high operating temperatures. Particularly, the impact of temperature has a great influence on the battery behaviour during acceleration and regenerative braking events [36,37].

In order to guarantee the long-term cycleability of the battery cells as much as possible, there is a need for a comprehensive study of the ageing phenomena in the battery at different operating conditions as listed in the previous section.

In [7,8,16–19], different battery chemistries have been investigated based on their performances. However, the analyses were only suitable to demonstrate the capability of the parameters such as energy, power, capacity and internal resistance.

From the point of view of the battery lifetime, in [29], the relevance of fast charging is reported and analyzed. The authors performed three similar tests at three working temperatures (0 °C, 25 °C and 40 °C). They concluded that battery energy efficiency decreases when the working temperature reduces. However, the combination of temperature and current rate change has not been investigated in literature. Furthermore, in [38–42], the main ageing parameters such as internal resistance increase and capacity fade in lithium-ion chemistries are analysed and discussed, based on half-cell levels. From the point of view of the "electrical approach", in [43], an analysis has been performed at two different working temperatures to analyse the power fade during the cycle life, relating this parameter to the state of health. The authors found that the power fade at 25 °C is less pronounced than its value at 45 °C. Particularly, the lithium nickel manganese cobalt oxide and lithium nickel cobalt aluminium have been analysed. Wright et al. [43] concluded that the relationship between the resistance increase and the storage time at specific temperature could be proposed as a square root.

In [44,45], the charge & discharge resistances of lithium nickel cobalt oxide battery cells have been investigated at various working temperatures (40 °C, 50 °C, 60 °C and 70 °C). The authors have applied the normal Hybrid Pulse Power Characterization (HPPC) test at 60% and 80% SoC during the cycle life of the battery. According to the performed analysis, a life cycle model has been extracted. However, one should pay attention that the maximum temperature for the proposed battery chemistry is 40 °C and 55 °C during charge and discharge, respectively. The presented analysis exceeds this envelope and cannot have occurred in reality. Ning et al. have extended the proposed analysis by performing cycles life test at different current rates (1 I_t, [1] 2 I_t and 3 I_t) [45]. They found that capacity decrease at 300 cycles is around 9.5%, 13.2% and 16.9% for 1 I_t, 2 I_t and 3 I_t, respectively. Moreover, they concluded that internal resistance has its largest value at 3 I_t.

In [46], Wang et al. performed accelerated cycle life tests at different conditions such as DoD and temperature. From the experimental results, a test matrix has been built. From this matrix, mathematical expressions have been derived illustrating the battery lifetime. However, this analysis has been carried out at low current rates. Further, the authors used the Arrhenius law for interpolation and extrapolation of the battery lifetime versus working temperature.

Following this work, the researchers of ISEA performed an accelerated lifetime tests at different working temperatures and SoC levels for obtaining a mathematical relationship between the storage time, temperature and voltage on ageing [47]. The developed model seems interesting to investigate the impact of the mentioned parameter on the battery lifetime. However, this study should be extended at different working conditions and the model needs then to be adjusted. Here, it should be underlined that only nickel manganese cobalt oxide batteries have been used in this study, which may thus not be extrapolated to the other battery chemistries.

Following this research, Kassem et al. carried out a similar analysis on lithium iron phosphate based batteries at three different temperatures (30 °C, 45 °C, 60 °C) and at three storage charge conditions (30%, 65%, 100% SoC). They observed that the capacity fade increases faster with the storage temperature compared to the state of charge [48]. Moreover, they concluded that lithium loss has been identified as the main source of the capacity fade. The capacity fade comes up from side reactions at the anode. While at cathode level, the loss is less prominent.

Amine et al. [49] concluded that the capacity fade at high temperatures was related to the dissolution of Fe^{2+} from the $LiFePO_4$ electrode and subsequent deposition of the ions on the carbon electrode, where the metal deposit tends to catalyze the formation of the solid–electrolyte interface (SEI) layer. Moreover, the formation of the SEI layer is responsible for the lithium-ions consumption and the increase of the high surface resistance and reduction of the available capacity. These results also have been confirmed by Song et al. [50]. They observed that cycling the battery at 25 °C temperature is less pronounced than at 55 °C. The capacity fade after 600 cycles at 25 °C was 5% compared to 30% at 55 °C.

A lifetime model has been developed based on a static experimental analysis at various SoC conditions and temperatures [51]. The developed model for lithium iron batteries is showing quite good results compared to experimental results but at low SoC levels the model is not accurate enough. In the proposed article, the model is more interesting for stationary applications. However in HEVs and BEVs, there is a need to perform a more dynamic analysis, which is representative to the battery behaviour in such vehicles. Moreover, in [52] it is indicated that the most relevant parameters in BEVs are the storage temperatures, depth of discharge, current rates and fast charging.

All this research shows the need for a complete analysis of the ageing electrical parameters of lithium-ion battery based on non-accelerated conditions as have been done in [46,47]. Therefore, the battery should be tested under a realistic load profile that is usual in BEV applications instead of using a constant current profile.

Furthermore, such analysis will allow the battery designer to have a clear view of the main changing parameter inside the battery, which can further be related to the SoH estimation. Moreover, based on such analysis all needed empirical relationships further will be used for development of a cycle life model.

2. Test methodology

In this paper, a novel methodology is proposed as presented by Fig. 1 for analysis of the main ageing parameter in lithium iron phosphate based batteries. The proposed approach differs on several levels from the existing works in the literature and the advantages are many-folds:

- The existing works are mostly related to some specific performance parameters, which do not reflect all ageing phenomena in lithium-ion batteries. But, our approach is extended as illustrated in Fig. 1, whereby the cycleability of the proposed battery has been investigated at different conditions such as operating temperature (40 °C, 25 °C, 0 °C, −18 °C), depth of discharge (100%, 80%, 60%, 40%, 20%), discharge current rates (1 I_t, 5 I_t,

[1] The current I_t represents the discharge current in amperes during 1 h discharge and C is the measured capacity of a cell as specified in the standard IEC 61434 [22,23].

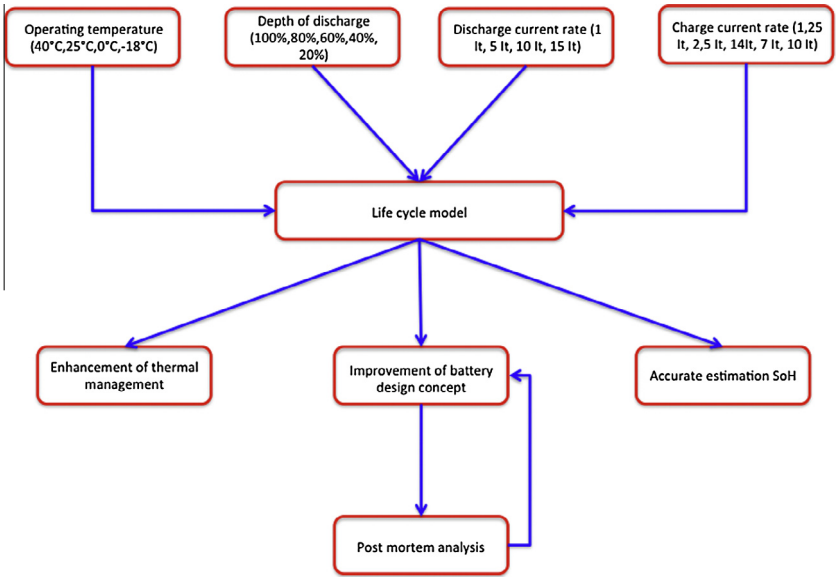

Fig. 1. Test methodology.

10 I_t, 15 I_t) and charge current rates (1.25 I_t, 2,5 I_t, 4 I_t, 7 I_t, 10 I_t). The cycleability of the battery at these conditions will provide the required information regarding fading mechanisms. The execution of a test methodology at such large-scale is a novel method and has not been performed before.

- The performed analysis has been mainly done at a standardized dynamic load profile as presented by Fig. 2 [53], which represents the battery behaviour in BEVs compared to the constant profiles in the existing works. Then, these tests have been performed based on non-accelerated conditions compared to the existing works, whereby the batteries have been investigated at accelerated conditions [46,47].
- The standard specifies that the cell should be subjected to the micro-cycle (see Fig. 2) until the depth of discharge capacity is 80%, after which the cell will be fully charged. This process of charging and discharging will continue until the cell capacity at "1 I_t" has reached 80% of the initial capacity.
- The standard specifies that the test should be performed at 45 °C in order to accelerate the ageing mechanism of the battery. However, the numbers of commercial lithium-ion batteries that can operate at this charge temperature are very limited. For most batteries, the maximum charge temperature is 40 °C. Cycling the cells (or battery) at high temperature can lead to damage the battery. The results that can be obtained from the mentioned test are not relevant to compare the batteries to each other due to the fact that the cycle life of the cells as specified by the manufacturer are derived at room temperature. The standard proposes to convert the obtained cycle life value at 45 °C into a calculated value at room temperature by using the Arrhenius law. However, the Arrhenius law can only be used in the cases when the system is exponential. Due to the fact that the Li-Ion cells do not show a strictly exponential characteristic, the obtained value according to the standard will not represent a realistic value.
- In this study, the depth of discharge has been extended till 100% instead of 80% as a typical worst-case scenario for BEV and PHEV applications. The micro-cycles of ISO 12405-2 have been used, calibrated in current rates instead of power rates however. The maximum employed discharge current pulse is 4 I_t.
- In this study, all the experimental tests have been conducted simultaneously using the battery tester PEC Corporation SBT 0550 and the climate chamber CTS C-40/350 [54,55].
- Most of the existing works are related to a specific lithium-ion chemistry (mostly NMC). However, the performances and aging mechanisms in this battery chemistry differ from the LFP batteries. This means that the analyses cannot be generalized. Therefore, there is a need for having extended aging investigation on other lithium-ion batteries (e.g. LFP batteries) [43–45,47].
- The proposed approach provide a clear view regarding the change of the internal resistance and capacity fade at different conditions, which can be assumed as a key parameters for estimation of SoH of batteries.
- Then, our approach also gives all the mathematical relationships for development of a life cycle model. Thus, the model can be used for prediction of the battery cycleability at different conditions in contradiction to the most existing works, whereby the analyses have been done at specific conditions and for specific applications [51].
- The developed model has further the advantage, which can support the battery designer to optimize the battery design concept. It means that the battery manufacturer can improve its battery at specific conditions, where the previous battery did not performed well.
- The approach also provides the required information regarding the heat development in the battery. It means that the cooling in the battery system should be designed to remove the heat from the system.

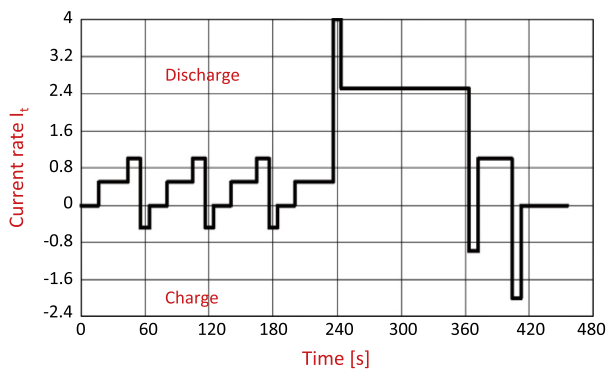

Fig. 2. Charge-depleting micro-cycle [53].

- In this manuscript, an analysis is included regarding battery performances at different charge regimes. This analysis is a novel methodology and has not been proposed in the literature. The executed work is proposed to develop dedicated control algorithms for charging the battery, whereby high performances and fast charging can be combined.
- In the last years, this issue becomes a hot topic in the field of batteries and development of charging systems for electric vehicles.
- Finally, the development of lithium-ion batteries performs at a high speed, whereby batteries continuously become improved in terms of coating systems, new electrodes, change in morphology of the electrode, new electrolyte. This result to the fact that execution of ageing analysis for all batteries still remain a key issue in the scientific community.

Here it should be underlined that ageing phenomena based on the calendar life and post mortem analysis are out of the scope of this article.

These performed tests have been performed on cylindrical lithium iron phosphate based battery type (2.3 Ah, 3.3 V). The electrode materials of the proposed battery are lithium iron phosphate in the positive electrode and graphite in the negative electrode. The battery has an energy density about 98 Wh/kg and a discharge power performance about 1800 W/kg at 50% SoC and room temperature (23–25 °C) during a pulse of 10 s [30,36].

In this analysis, 3 battery cells have been used at each working conditions. The presented results below are the average results.

It should be pointed out that the ageing study has been performed from the point of view of "electrical approach".

3. Results and discussions

3.1. Working temperature

In order to assess the impact of the working temperature behaviour on the battery long time performances, cycle life tests have been carried out at specified ambient temperatures: 40 °C, 25 °C, 0 °C, −18 °C. The battery cells have been charged, at constant current 1 I_t followed by constant voltage 3.6 V until the current reached the specified end value (0.01 I_t). Then, the battery cells get a break time of 30 min. Thereafter, the batteries are subjected to the load profile as proposed in Fig. 2. When the cut-off voltage (2 V) has been reached, the battery cells are charged again followed by a break time of 30 min.

At each 50 cycles, the battery cells have been submitted to a capacity test at 1 I_t for analysis of the remaining capacity in the battery cell. At the end of this test, a discharge pulse of 5A during 100 ms at 100% SoC has been imposed for determination of the internal resistance. This procedure is a standard test in the mentioned battery tester.

Before starting the test, cells were conditioned at the proposed working temperatures during 6 h. During the cycle life test, the surface temperature of the battery cells have been measured by placing a thermal sensor (type *K* thermocouple) in the middle of the battery cell surface as to avoid exceeding the maximum allowed temperature as defined by the battery manufacturer.

In Fig. 3, the evolution of cycle number is illustrated in function of operating temperature. The end-of-life criterion is 80% of the original capacity under standard conditions. As can be observed from Fig. 3, the evolution can be described by a polynomial equation of 3th order. This empirical relationship, which can b fitted by using the least-square fitting method:

$$\mathrm{CL} = a.T^3 - b.T^2 + c.T + d \quad (1)$$

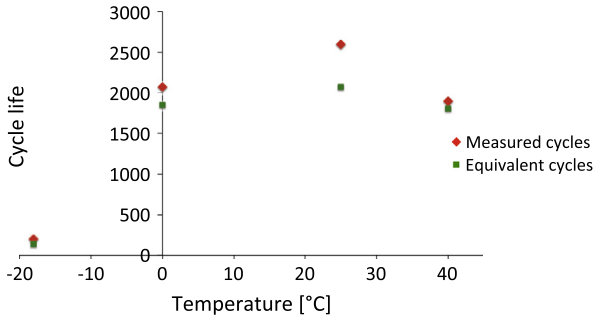

Fig. 3. Evolution of cycle life versus working temperature.

where CL: cycle life of the battery; *T*: the operating temperature (°C).

Fig. 3 shows that the lifetime of the battery decreases above 25 °C. The reason for this evolution is due to instability of the solid electrolyte interface (SEI) [39,49,50,56]. At each charge cycle, the SEI will consume some Li extracted from the LFP at the graphite surface for making the Li containing inactive species. Due to such phenomena:

- the consumption of Li, which is contributing for reversible capacity will be less,
- the internal resistance at the graphite surface will increase continuously,
- the capacity fade in the battery increases,
- a misbalance occurs in the electrochemical process of the battery whereby the cycle life decreases.

The above results at elevated temperature have also been confirmed by Ramdass et al. [57]. They concluded that after 800 cycles, the considered lithium iron phosphate based batteries at room temperature and 45 °C showed 30% and 36% capacity fade, respectively, due to the faster increase of the internal resistance on the positive electrode at 45 °C against at room temperature. The less beneficial cycle life results at low temperatures have been related to the formation of the lithium plating [39].

In order to have beneficial battery performances during the long term, the batteries should be kept in the operating temperature 15–35 °C, where the increase of the internal resistance in this region is limited compared to its value at 40 °C (127%) and −18 °C (till 135%) as illustrated in Fig. 3. The increase of the internal resistance will not only have a negative impact on the battery performances (power fade), but also on the energy efficiency of the battery. This will further increase the temperature raise in the cells, which will further increase and accelerate the ageing phenomena in the battery as one can observe from Fig. 3. In addition, this aspect will be significant for the dimensioning of the cooling system in the battery system.

The results at 25 °C have more or less been confirmed by Waag et al. [58]. However, it should be noted that their investigation has been carried out on lithium nickel manganese cobalt based batteries.

The standard ISO 12405-2 defines battery end of life when the discharge capacity is reduced to 80% of the initial capacity. From this point of view, one can conclude that the state of health (SoH) of a battery can be related to the capacity decrease as it is presented by Eq. (2).

$$\mathrm{SoH} = \frac{C_{\mathrm{dis,act}}}{C_{\mathrm{dis,init}}} \quad (2)$$

where $C_{\mathrm{dis,act}}$, the actual discharge capacity of the battery (Ah); $C_{\mathrm{dis,init}}$, the initial discharge capacity of the battery (Ah).

As shown in Fig. 4, the increase of the internal resistance of the battery can also be assumed a crucial parameter for definition of the state of health. This increase is more pronounced at 40 °C and −18 °C than at 25 °C. Therefore, Eq. (2) can be proposed by partial differential relationship:

$$\mathrm{dSoH} = \frac{\partial \mathrm{SoH}}{\partial C_{\mathrm{dis,act}}} dC_{\mathrm{dis,act}} + \frac{\partial \mathrm{SoH}}{\partial R_{b,\mathrm{incr}}} dR_{b,\mathrm{incr}} \quad (3)$$

where $R_{b,\mathrm{incr}}$, is the increase of the internal resistance of the battery (Ω).

According to these results, we can observe that the well-known FreedomCar battery model should be adapted whereby the impact of the internal resistance increase can be taken into account as presented in Fig. 5. As we can see, the presented battery model takes into account the hysteresis of the battery as illustrated in Fig. 6. The hysteresis has been included by separating the charge and discharge ohmic resistances ($R_{o,ch}$, $R_{o,dis}$) and the RC polarization circuits. Then, the model has been enhanced by including two separate ohmic resistances during charge and discharge ($R_{LC,c}$, $R_{LC,dis}$), which represent the evolution of the resistance during its cycle life. The same issue has been performed regarding the RC circuits. Based on the latter two modifications, the SoH estimation can be proposed as function of the sum of the ohmic and polarization resistances.

From the point of view of capacity and state of charge (SoC) evolution, the situation seems less beneficial. The shape of the SoC curves strongly varies in function of the working temperature and the cycle life as can be derived from Fig. 7. From this figure, one can observe that the battery is degrading in function of the cycle life, the battery discharge capacity decreasing. From this evolution, one can conclude that there is a need for a modification of the term cycle life. At working temperatures −18 °C where the internal resistance is high due to the low conductivity, the total accumulated capacity (Ah) is less compared to at working temperature 25 °C [47,52]. Therefore, it is more appropriate to define an equivalent cycle (CL_{eq}) where the effective cycle of a battery can be calculated independent of the working temperature. Based on this methodology, one can calculate the cycle life of a battery based on a well-defined capacity. In this study, the measured begin of life (BoL) of the battery capacity at 25 °C has been selected as the reference capacity.

$$CL_{eq} = \frac{C_{\mathrm{dis,act}}}{C_{\mathrm{ref}}} \quad (4)$$

where CL_{eq}, is the equivalent cycle; $C_{\mathrm{dis,act}}$, is the accumulated net discharge capacity during cycle life (Ah); C_{ref}, is the measured discharge battery capacity at 25 °C and at BoL (Ah).

From Fig. 3, we recognize that the equivalent cycles at 25 °C (2071 cycles) and 0 °C (1850 cycles) are smaller compared to 2600 at 25 °C and 2070 measured cycles at 0 °C, respectively. This methodology allows us to calculate the effective number of cycles that a battery can achieve based on a fixed driving range.

Finally, based on Fig. 7, one can observe that the association of state of charge to a reference voltage evolution will have dramatic consequences on the accuracy of the SoC prediction. Due to the degradation of the battery, the voltage evolution changes strongly in function of the cycle life. The voltage reading can thus not be considered a good solution for SoC estimation.

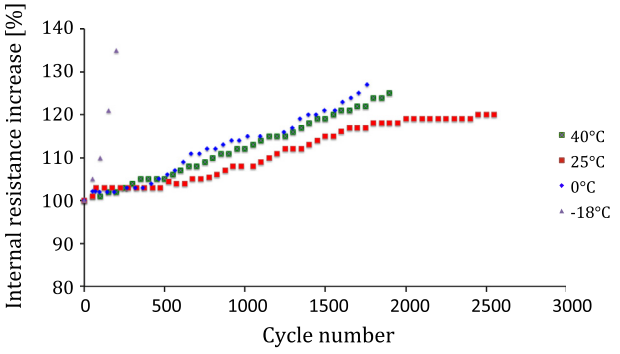

Fig. 4. Increase of internal resistance versus cycle number.

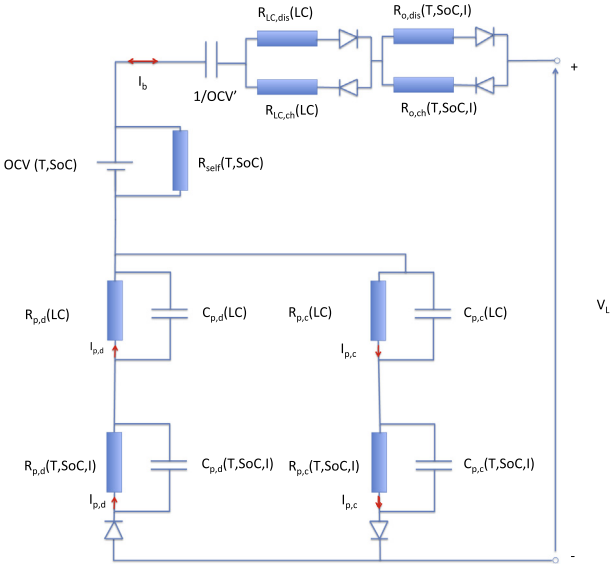

Fig. 5. Advanced second order FreedomCar battery model.

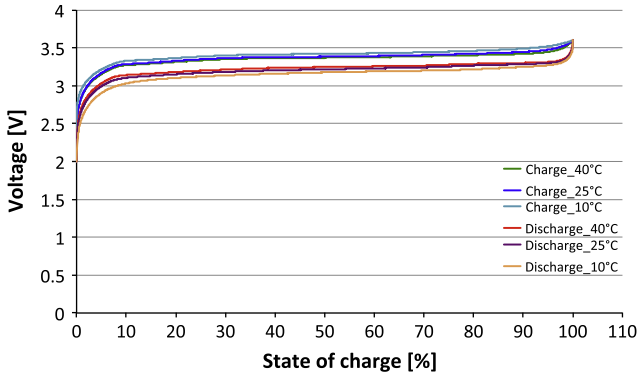

Fig. 6. Hysteresis of the investigated battery cells.

3.2. Constant discharge current rates

In the previous Section 3.1, the cycle life tests have been performed at a well-defined dynamic load profile. This profile does not include the impact of current rate change on the battery performances. In order to take this issue into account in the analysis of the ageing phenomena, there is a need for an additional test at different constant discharge current rates. Therefore, a series of cycle life tests have been carried out at constant currents 1 I_t, 5 I_t, 10 I_t, 15 I_t and at room temperature till 100% DoD.

Here it should be noted that the battery cells have been charged at the same procedures as defined in Section 3.1.

Fig. 8 shows the results of the remaining capacity in function of cycle life, with a much faster capacity decrease at high current rates. The lifetime of the battery is 2900, 2060, 1100 and 560 cycles at 1 I_t, 5 I_t, 10 I_t and 15 I_t, respectively.

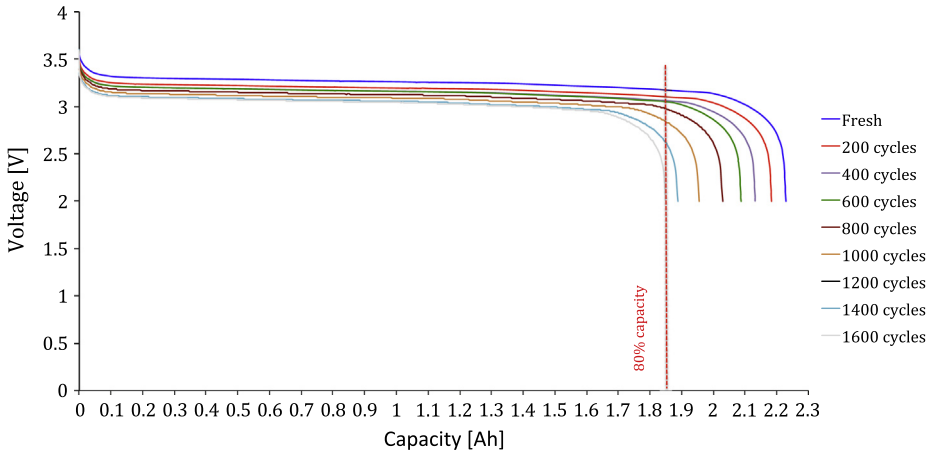

Fig. 7. Evolution of voltage versus capacity at during cycle life at 40 °C working temperature.

Moreover, based on the evolution of the cycle life duration current rate, the following mathematical expression has been derived based on the least square fitting method in Matlab Simulink.

$$\mathrm{CL}(I_d) = e.e^{(f.I_d)} + g.e^{(h.I_d)} \tag{5}$$

Ning et al. reported that the fast capacity degradation of the battery at high discharge current rates is due to the change in the carbon structure [45]. This has been illustrated based on a number of cycle life tests at 1 I_t, 2 I_t and 3 I_t, showing capacity degradations after 300 cycles of 9.5%, 13.2% and 16.9% respectively. Furthermore, based on scanning electron microscopy (SEM) images, they did not observe significant structure change at the carbon electrode surface at 1 I_t. However, at 2 I_t and 3 I_t the structure exhibits more white substance and cracks on the surface. Following this reference, the researchers of university of Aarhus concluded that the battery performances of optimized lithium energy battery decreases the more the current rates increases [59]. They observed that the internal resistance increases with the current rate. This observation has been obtained based on impedance spectroscopy analysis.

Furthermore, during the cycling test, the surface battery temperature of the battery cells has been monitored by using thermal sensors (Type *K*) in the middle of the battery cells. From the experimental results, one can observe that the high surface temperature at 10 I_t and 15 I_t (about 55 °C).

From Fig. 8, one can conclude that the battery performance decreases the more the battery temperature raises. However, in this case the capacity retention is much faster due to the combination

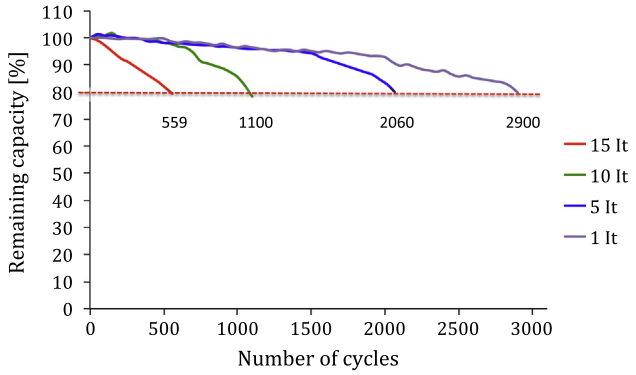

Fig. 8. Evolution of remaining capacity versus cycle life at different current rate.

of the high battery temperature and applied current rates. These observations have also been confirmed in Refs. [47,48,60–65].

The high surface temperatures at 10 I_t and 15 I_t are due to the higher resistance losses in the battery as presented by Eq. (6):

$$E_{\mathrm{loss}} = \int R_b \cdot I_b^2 \cdot dt \tag{6}$$

where E_{loss}, is the resistance loss (J); R_b, is the battery resistance (Ω); I_b, is the current that flows through the battery (A).

The internal resistance and high current rates result in increasing of the Joule losses in the battery, which translates in a high surface temperature. In Fig. 9, we recognize that the internal resistance at 10 I_t and 15 I_t increases faster than its value at 1 I_t current rate. The internal resistance increase is 123%, 132%, 156% and 140% at 1 I_t, 5 I_t, 10 I_t and 15 I_t current rates, respectively.

Ning et al. concluded that the considerable high increase of the internal resistance at high current rates is due to the cracks that result to formation of a new SEI layer [45]. This layer becomes thicker during the cycle life of the battery. This results in a significant increase of the internal resistance of the battery cell.

Here, it should be noted that the surface temperature at 15 I_t reached the maximum allowed discharge temperature as specified by the battery manufacturer (60 °C). Therefore, the battery cells at 15 I_t have been cooled by using a conventional fan, and the temperature at 15 I_t represents the surface temperature when the battery cells are cooled by the fan. The temperature after cooling is thus still in the range as at 10 I_t.

Finally, in Fig. 10, the Peukert[2] number has been calculated during the lifetime of the battery. This figure confirms the discharge rate capabilities of the battery when the battery is continuously discharged at 10 I_t and 15 I_t current rates. The Peukert number increases to 1.018, 1.035, 1.044 and 1.052 at 1 I_t, 5 I_t, 10 I_t and 15 I_t current rates, respectively. At every 50 cycles, the Peukert number has been determined based on 1 I_t and 5 I_t from 100% till 0% state of charge.

[2] Peukert phenomenon is an empirical formula which approximates how the available capacity of a battery changes according to the rate of discharge as expressed by the following equation [69]:

$$C_p = T_{\mathrm{dis}}, I_{b,\mathrm{dis}}^k$$

where C_p is the theoretical capacity of the battery expressed in Ah, I_{dis} is the discharge current, T_{dis} the discharge time and k is the Peukert number. This equation shows that at higher discharge current, there is less available capacity in the battery. The Peukert number indicates how well a battery performs under continuous heavy discharge current. A value close to 1 indicates that the battery performs well; the higher the value, the more capacity is lost when the battery is discharged at high current.

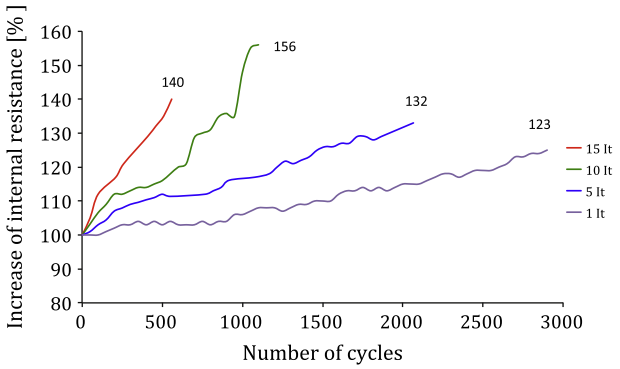

Fig. 9. Increase of internal resistance versus cycle life.

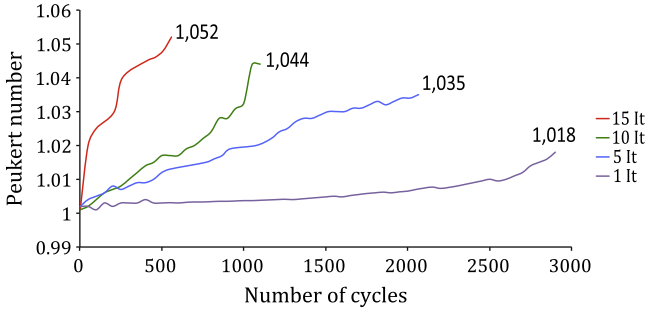

Fig. 10. Peukert evolution versus cycle life at different current rates.

From this analysis one can conclude that the combination of high temperatures and high current rates is very harmful for the performances of a battery.

Furthermore, one can conclude that the Peukert number can be considered as a key parameter for the assessment of the state of health of the battery.

3.3. Depth of discharge

In the previous Sections 3.1 and 3.2, the impacts of the working temperature and constant discharge current rate on the battery performances have been illustrated and analysed. However, all these tests have been carried out until 100% depth of discharge (DoD). In real-life BEV applications, the battery is never depleted completely, with SoC varying between 100% and 30%.

In [66], Rosenkranz et al. made a comparison of the cycle life of various battery technologies in function of DoD. From this test, mathematical relationships have been extracted. The analysis shows that the evolution of the cycle life is not fixed. It is a strongly battery technology dependent. They assumed that the relationship of the cycle life versus DoD for all lithium-ion battery chemistries should be the same. However, the results in [67] indicate that the battery performances change in function of many parameters such as (temperature, current rate, DoD). In addition, the results are strongly chemistry dependent. Following to this work, Schaltz illustrated the evolution of cycle of lithium-ion battery in function of DoD based on battery manufacturer data [68].

Based on these references, there is a need to perform a cycle life analysis in function of DoD based on a realistic load profile and not at constant currents as reported in [66,68,71].

In order to have a clear view of the battery performances at different SoC levels and for extraction of a relationship for modeling purposes, a series of cycle life tests have been performed at 20%, 40%, 60%, 80% and 100% DoD at room temperature (20–25 °C). Therefore, the same load profile has been used as presented in Fig. 2 in Section 2 "Test methodology".

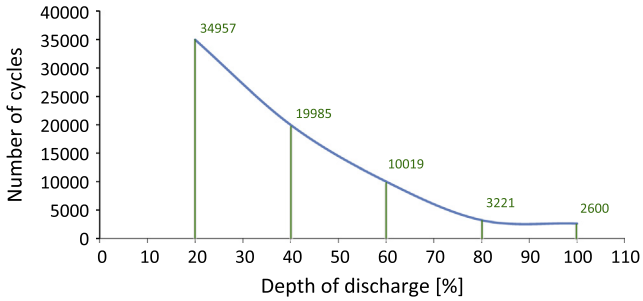

Fig. 11. Evolution of cycle versus depth of discharge.

The batteries were fully charged as described in Section 3.1 and have been discharged till the cut-off voltage[3] is reached. The measured net dynamic discharge capacity corresponds to the battery capacity in the beginning of life. This value is also equal with 100% DoD. The net discharge capacity was also measured at 20%, 35%, 50%, 65% and 80% DoD.

The end of life has of the battery cells has been determined by performing a standard cycle[4] until 100% DoD every 200 cycles, to determine the total discharge capacity of the cell.

In Fig. 11, the results of the above analysis are presented. The cycle life evolution is assumed as an exponential function as presented by (7). The proposed empirical relationship has been derived by using least-square fitting method as discussed in Section 3.1.

$$\mathrm{CL}(\mathrm{DoD}) = i.e^{(j.\mathrm{DoD})} + k.e^{(l.\mathrm{DoD})} \quad (7)$$

From the experimental results, one can conclude that the battery cell is able to perform 3221 deep cycles (till 80% DoD) compared to 34957 shallow cycles (till 20% DoD).

According to the USABC goals, the battery should be able to perform 300,000 shallow cycles during charge sustaining mode [37]. By comparing this objective with the obtained results, one can conclude that the USABC objective is rather ambitious.

According to Rosenkranz [67], the lithium-ion batteries in PHEVs should be able to perform about 15,000 cycles (till 20% DoD). This result seems below the obtained results from this study. A possible reason could be that the investigated batteries by Rosenkranz were optimized for high-energy applications [67], while the used battery cell in this paper has more power capabilities. Furthermore, Rosenkranz did not specified the conditions of the tests that have been performed.

Fig. 12 shows the increase of internal resistance during cycle life, based on the internal resistance method as described in Section 3.1, with an internal resistance increase much higher at deep discharge. Particularly, for 100% DoD, the internal resistance increase is significantly higher at about 132% compared to 126%, 119%, 116%, 112% for 80%, 60%, 40% and 20% DoD, respectively. This test indicates that the increase of internal resistance is one of the stress factors in the battery as observed in Fig. 4. In addition, this analysis confirms again that the internal resistance of the battery has a great influence on the battery performance and should be taken into account as a major assessment parameter for SoH determination.

[3] Cut-off voltage is the minimum battery voltage as specified by the battery manufacturer.

[4] Standard cycle exists of a standard constant current/constant voltage charge method as described in Section 3.1 following by a standard discharge current at 1 I_t till cut-off voltage.

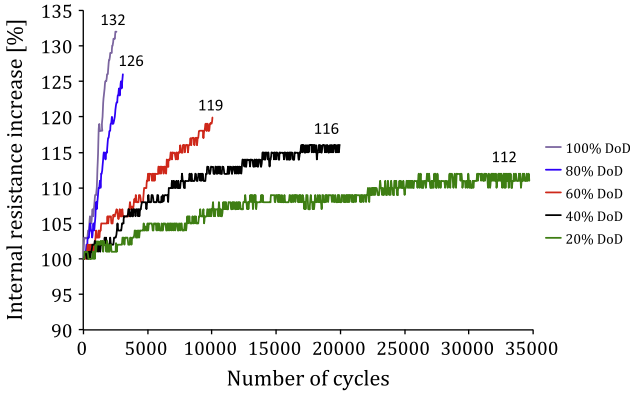

Fig. 12. Evolution of internal resistance versus number of cycles.

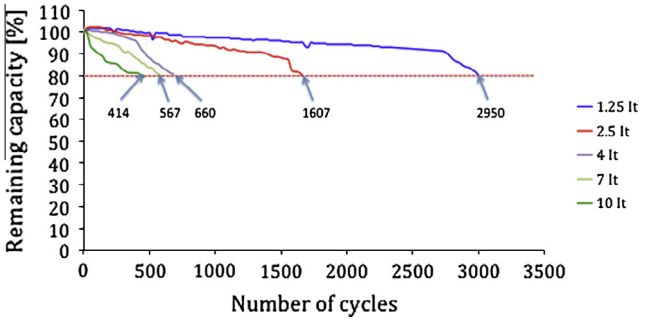

Fig. 14. Evolution of capacity decrease versus number of cycles.

In order to illustrate the battery ageing behaviour in depth, the Peukert number as analysed in [70] has been calculated based on discharge current rates 1 I_t and 5 I_t.

Fig. 13 indicates the same evolution as well as Fig. 10. The Peukert number increases the more the battery is deeply discharged. Particularly, at 100% DoD, the increase of Peukert is more pronounced (1.045), while the evolution of Peukert number at 20% DoD is less and more stable.

Table 1
Charging rates at various power levels.

Charging power (kW)	Charging time (h)	Battery current (A)	Current rate (I_t)
3	8	10	0.125
6	4	20	0.25
12	2	40	0.5
24	1	80	1
48	0.5	160	2
96	0.25	320	4

3.4. Fast charging

In battery electric and Plug-in Hybrid Electric Vehicles, fast charging capability is considered a desirable trait.

In [53], the performances of different lithium-ion batteries with various chemistries have been analysed at several charge current rates. The authors concluded that high power optimized battery cells can absorb considerably high currents. Following to this work, in [30], Patel et al. performed a series of capacity tests at different charge current rates and operating temperature on a high capacity lithium iron phosphate battery. They concluded that the stored capacity in the battery is strongly dependent of the applied current and the ambient temperature due to the change of the internal resistance. However, the impact of the high load on the battery behaviour during the long term was not analysed. Moreover, Ansean et al. performed an extended cycle life test analysis on the same battery cells as proposed in this article in order to investigate the impact of the charge current rate on the battery performances [72]. In this article, a comparative study has been carried out based on 3 different load profiles: 1 I_t during charging and discharging, dynamic load profile and fast charging at 4 I_t. The authors concluded that the impact of charging current is independent on the battery performances.

However, in [73] is documented that the degradation of EV batteries is sensitive to charging regime for bulk energy services. From these references, we can observe that the evolution of the battery as function of the cycle life is still unclear.

In order to have a clear view inside the battery charge capabilities, a number of cycle life tests have been carried out at constant charge current rates 1.25 I_t, 2.5 I_t, 4 I_t, 7 I_t and 10 I_t and at room temperature (20–25 °C). The cells were discharged beforehand with 1 I_t at room temperature. The discharging process ends when the cut-off voltage is reached. Then, the battery gets a rest time of 30 min before starting with the following charging procedure as specified in Section 3.1.

In order to investigate the capacity decrease of the battery, at every 20 cycles the battery cells have been subjected to a standard cycle, whereby the battery cells have been charged at the same way as reported in Section 3.1 and discharged at 1 I_t current rate till cut-off voltage has been reached. The standard cycle is needed to observe when the battery capacity has reached the end of life.

In Fig. 14, the battery cell capacity at different charging current rates is illustrated. Fig. 14 shows that the cycle life of a battery is strongly dependent on the applied charging current rate. The cycle life of the battery decreases from 2950 cycles to just 414 at 10 I_t. From this analysis, one can conclude that the studied lithium-ion battery cells are not recommended to be charged at high current rates. Furthermore, these results indicate the contrary of the obtained results by Ansean [72]. The main reason for the obtained evolution is related to the formation of lithium plating at high

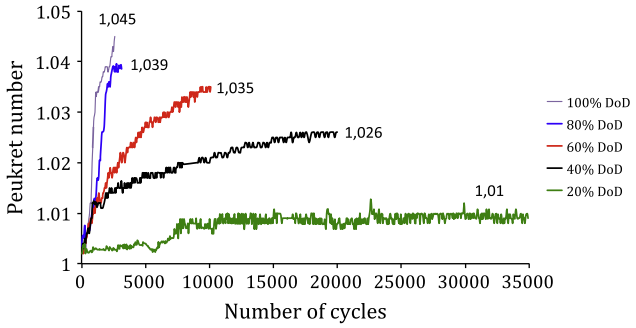

Fig. 13. Evolution of Peukert number versus cycle life.

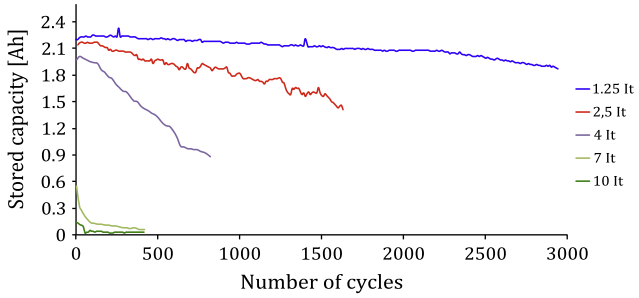

Fig. 15. Stored capacity versus cycle life.

Table 2
Summary of the extracted relationships at different working conditions.

Relationships	Coefficients			
Cycle life versus working temperature	a	b	c	d
$CL = a.T^3 - b.T^2 + c.T + d$	0.0039	1.95	67.51	2070
Cycle life versus constant discharge current rates	e	f	g	h
$CL(I_d) = e.e^{(f.I_d)} + g.e^{(h.I_d)}$	4464	−0.1382	−1519	−0.4305
Cycle life versus depth of discharge	i	j	k	l
$CL(DoD) = i.e.^{(j.DoD)} + k.d^{(l.DoD)}$	6.009.e9	−0.011879	6.009.e9	−0.01879
Cycle life versus constant charge current rates	m	n	o	P
$CL(I_{ch}) = m.e^{n.I_{ch}} + o.e^{(p.I_{ch})}$	5963	−0.6531	321.4	0.03168

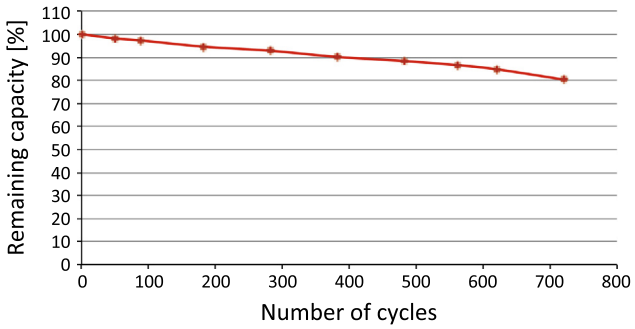

Fig. 16. Evolution of the battery remaining capacity versus cycle life based on experimental results.

current rates [40,74,75]. This process is not fully reversible where lithium ions form metallic lithium at the surface instead of the intended intercalation. This results into decrease of the active material and further degradation of the battery capacity. This process accelerates the more the charge current rates increases as we can observe in Fig. 14.

This means that the fast charge systems as presented in [76] will not have a positive impact on the battery systems using such cells and that the real usefulness of extremely fast charging (7 I_t and higher) has to be reconsidered notwithstanding that it is already a high power cell.

Based on the evolution of the battery capacity degradation as function of the charge current rate, Eq. (8) has been extracted by using the Matlab/Simulink least-square fitting method. As we can observe, the evolution of the life cycle as function of the charge current rate is exponential.

$$\mathrm{CL}(I_{ch}) = m.e^{(n.I_{ch})} + o.e^{(p.I_{ch})} \tag{8}$$

To bring these figures in context, one can consider a typical electric vehicle, fitted with a 300 V, 80 Ah battery, with 24 kW h energy content. The actual charge rate of the battery (assuming the charge voltage constant and discounting all losses in the charger) for various charging power levels would be as illustrated in Table 1. It becomes clear that the so-called "semi-fast" charging rates up to 24 kW [77] are acceptable, but extremely fast charging is not.

Furthermore, the stored charge capacity during the cycle life has been recorded as presented in Fig. 15. As can be observe from the obtained results, the stored capacity is strongly dependent on the applied charging current rate. The limited stored capacity at high current rates is due to the high voltage drop. The voltage drop becomes during the cycle life test higher than other cases due to the increase of the internal resistance. Therefore, the stored capacity decreases as it is illustrated in Fig. 15.

4. Development of a cycle life model

In the design and selection of rechargeable energy storage systems, a simulation model can be an interesting tool for assessing the system behaviour during short and long term [45–47]. In this paper, a cycle life model has been developed based on the evolution of the cycle life as function of the parameters working temperature, constant discharge current rates, depth of discharge and constant fast charging as presented by Eqs. (1), (5), (7) and (8). In Table 2, a summary is given of the extracted equations and their coefficients. The extractions of the equations and coefficients have been done based on the least square fitting method.

All these relationships have been integrated in Matlab Simulink for having a general cycle life model at the proposed working conditions.

In order to validate the accuracy of the model a validation test has been performed at room temperature at 4 I_t constant charging current as specified in the Section 3.1 and then discharging at 4 I_t until the cut-off voltage (2 V) has been reached. In order to accelerate the conditions, the rest time between charging and discharging phases has been fixed on 10 min.

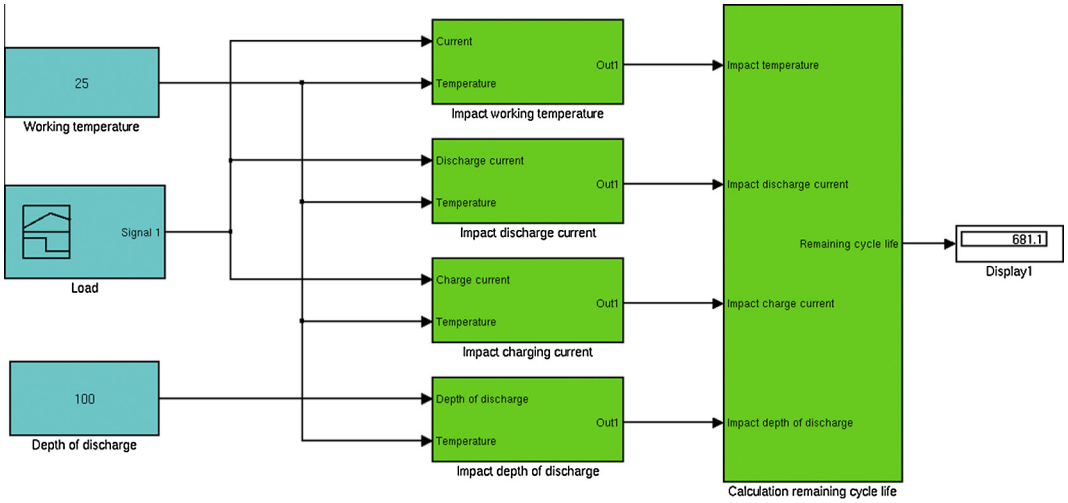

Fig. 17. Overview of the developed cycle life model.

According to the experimental results, the battery is able to perform 720 cycles (see Fig. 16) against 681 cycles (see Fig. 17) based on simulation results.

Bases on this validation result, we can conclude that the error between the simulation and the experimental results is smaller than 5.4%.

Here it should be underlined that the developed model has several advantages over the existing models in the literature [45–47]:

- The model has been developed based on significant numbers of performance parameters.
- The model has a relatively high acceptable accuracy, which indicates that the model can be used for control strategy purposes in advance when a vehicle will be developed. This issue will accelerate the development speed of the battery system and the battery lifetime can be extended by avoiding extreme operating regimes to the battery.
- The model can play a vital role in the development of thermal management, where the main focus is to keep the battery in the most appropriate operating range for having high performances and long cycle life.
- Then, the model can play an important role in the development an accurate estimation of SoH, which is a important parameter in the field of batteries,
- Further, the model could be a useful tool for the battery designers to improve the performances of their batteries in specific operating conditions,
- Finally, the model has been implemented in Matlab/Simulink environment as presented in Fig. 17, which can be integrated in any battery management system.

5. Conclusions

This paper describes a novel approach for assessment of ageing parameters in lithium iron phosphate based batteries. Battery cells have been investigated based on different current rates, working temperatures and depths of discharge. Furthermore, the battery performances during the fast charging have been analysed.

The investigated parameters are internal resistance evolution, capacity retention, Peukert number evolution and temperature evolution.

From the analysis, one can observe that the operating temperature has a great influence on the performance and lifespan of the battery. At elevated temperature (40 °C), the performances are less compared to at 25 °C.

The non-linear behaviour of the battery during the cycle life makes that the Arrhenius law cannot be applied to derive the battery lifetime from one temperature to another.

The influence of different depth of discharge levels has been described in a mathematical relationship.

Cycle life tests have illustrated the long-term capabilities of the studied battery cells at different current rates, revealing the harmful impact of the high current rates on the battery performances, and particularly the fact that the studied lithium-ion battery cells are not recommended to be charged at high current rates.

The results have demonstrated that the internal resistance and capacity retention are the main electrical parameters to can be taken into account for prediction of state of health of a battery.

Finally, a life cycle model has been developed based on the obtained evolution of the cycle life as function of the investigated conditions.

Based on the validation test, the error percentage between the simulated and experimental results is maximum 5.4%.

6. Future work

In this article, an extended ageing analysis has been carried out based on the electrical approach. However, this methodology does not provide any information to the ageing phenomena on material level. Therefore, in the future work a post mortem analysis will be carried out on the used batteries at the mentioned working conditions. This analysis will study the influence on the level of electrode, electrolyte and separator.

References

[1] Van den Burgwal E, Maggetto G, Van Mierlo J, Gense R. Driving style and traffic measures influences vehicle emissions and fuel consumptions. J Automob Eng 2003;218:43–50.
[2] Van Mierlo J, Vereecken L, Maggetto G. How to define clean vehicles? Environmental impact rating of vehicles. Int J Automot Technol 2003;4:77–86.
[3] Van Mierlo J, Timmermans JM, Maggetto G. Environmental rating of vehicles with different alternative fuels and drive trains: a comparison of two approaches. J Transport Res D – Transport Environ 2004;9:387–99.
[4] Matheys J, Van Autenboer W, Timmermans JM. Influence of functional unit on the life cycle assessment of traction batteries. Int J Life Cycle Assess 2007;12:191–6.
[5] Maggetto G, Van Mierlo J. Fuel cell or battery: electric cars are the future. J Fuel Cells 2007;7:165–73.
[6] Maggetto G, Van Mierlo J, Vereecken L, Meyer S, Favrel V, Hecq W. Comparsion of the environment damage caused by vehicles with diferent alternative fuels and drive trains in a Brussels context. J Automob Eng 2003;217:583–93.
[7] Burke A, Miller M. Performance characteristics of lithium-ion batteries of various chemistries for plug-in hybrid vehicles. In: Proceedings EVS 24; 2009, Norway.
[8] Omar N, Daowd M, Verbrugge B, Mulder G, Van den Bossche P, Van Mierlo J, et al. Assessment of performance characteristics of lithium-ion batteries for PHEV vehicles applications based on a newly test methodology. In: Proceedings EVS 25; 2010, China.
[9] Chau KT, Chan CC. An overview of energy sources for electric vehicles. J Energy Conver Manage 1999;40:1021–39.
[10] Chau KT, Wang YS. Hybridization of energy sources in electric vehicles. J Energy Conver Manage 2001;42:1059–69.
[11] Van Mierlo J, Maggetto G, Lataire Ph. which energy source for road transport in the future? A comparison of battery, hybrid and fuel cell vehicles. J Energy Conver Manage 2006;47:2748–60.
[12] Silva C, Ross M, Fabrica T. Evaluation of energy consumption, emissions and cost of plug-in hybrid vehicles. J Energy Conver Manage 2009;56:1635.
[13] Emadi A, Williamson SS, Khaligh A. Power electronics intensive solutions for advanced electric, hybrid electric, and fuel cell vehicular power systems. IEEE Trans Power Electron 2006;21:567–77.
[14] Emadi A, Rajashekara K, Williamson SS, Lukic SM. Topological overview of hybrid electric and fuel cell vehicular power system architectures and configurations. IEEE Trans Vehicul Technol 2005;54:763–70.
[15] Lukic SM, Cao J, Bansal RC, Rodriguez F, Emadi A. Energy storage systems for automotive applications. IEEE Trans Ind Electron 2008;55:2258–67.
[16] Omar N, Verbrugge B, Mulder G, Van den Bossche P, Van Mierlo J, Daowd M, et al. Evaluation of performance characteristics of various lithium-ion batteries for use in BEV application. In: Proceedings VPPC; 2010, France.
[17] Omar N, Daowd M, Mulder G, Timmermans JM, Van den Bossche P, Van Mierlo J, et al. Assessment of performance of lithium iron phophate oxide, nickel manganese cobalt oxide and nickel cobalt aluminum oxide based cells for using in plug-in battery electric. In: Proceedings VPPC; 2011, USA.
[18] Omar N, Verbrugge B, Van den Bossche P, Van Mierlo J. Power and life enhancement of battery-electrical double-layer capacitor for hybrid electric and charge-depleting plug-in vehicle applications. Electrochim Acta 2011;55:7524–31.
[19] Omar N, Van Mulders F, Van Mierlo J, Van den Bossche P. Assessment of behaviour of super capacitor-battery system in heavy hybrid lift truck vehicles. J Asian Electric Vehicles 2009;7:1277–82.
[20] Omar N, Al Sakka M, Daowd M, Coosemans Th, Van Mierlo J, Van den Bossche P. Assessment of hebavior of active EDLC-Battery system in heavy hybrid charge depleting vehicles. In: Proceedings 4th European symposium on super capacitors & applications; 2010, France.
[21] Van Mierlo J, Timmermans JM, Maggetto G, Van den Bossche P. World Electric Vehicle Associat J 2007;1:54.
[22] Mulder G, Omar N, Pauwels S, Leemans F, Verbrugge B, De Nijs W, et al. Enhanced test methods to characterise automotive battery cells. J Power Sources 2011;196:10079–87.
[23] Omar N, Daowd M, Hegazy O, Mulder G, Timmermans JM, Coosemans Th, et al. Standardization work for BEV and HEV applications: critical appraisal of recent traction battery documents. Energies 2012;5:138–56.

[24] Burke A. R&D considerations for the performance and applications of electrochemical capacitors. Electrochim Acta 2007;53:1083–91.
[25] Kötz R, Carlen M. Principle and applications of electrochemical capacitors. Electrochim Acta 2000;45:2483–98.
[26] Daowd M, Omar N, Van den Bossche P, Van Mierlo J. Passive and active battery balancing comparison based on matlab simulation. In: Proceedings VPPC; 2011, USA.
[27] Axsen J, Burke A, Kurani K. Batteries for plug-in hybrid electric vehicles (PHEVs): goals and state of the technology, 2008, document number: UCD-ITS-RP-10-16; 2008.
[28] Van den Bossche P, Vergels F, Van Mierlo J, Matheys J, Van Autenboer W. SUBAT: an assessment of sustainable battery technology. J Power Sources 2006;162:913–9.
[29] Patel DD, Tredeau FP, Salameh ZM. Temperature effects on fast charging large format prismatic lithium iron phosphate cells. In: Proceedings VPPC; 2010, France.
[30] Mulder G, Omar N, Pauwels S, Meeus M, Leemans F, Verbrugge B, et al. Comparison of commercial battery cells in relation to material properties. Electrochim Acta 2012;87:473–88.
[31] Lukic SM, Wirasingha SG, Rodriguez F, Cao J, Emadi A. Power management of an ultra-capacitor/battery hybrid energy storage system in an HEV. In: Proceedings IEEE vehicular. Power Propulsion Conference; 2006, UK.
[32] Baisden AC, Emadi A. An ADVISOR based model of a battery and an ultra-capacitor energy source for hybrid electric vehicles. IEEE Trans Vehicular Technol 2004;53:199–205.
[33] Einhorn M, Valerio Conte F, Kral Ch, Fleigh J. Comparison, selection, and parameterization of electrical battery models for automotive applications. IEEE Trans Power Electron 2012;28:1429–37.
[34] Agarwal V. Development and validation of a battery model useful for discharging and charging power control and lifetime estimation. IEEE Trans Energy Conver 2010;25:821–35.
[35] Rogger JD. Characterization of li-ion batteries for intelligent management of distributed grid-connected storage. IEEE Trans Energy Conver 2011;26:256–63.
[36] Omar N. Assessment of rechargeable energy storage systems for plug-in hybrid electric vehicles. PhD thesis. Vrije Universiteit Brussel; 2012. ISBN: 978-94-6197-073-2.
[37] Omar N, Daowd M, Hegazy O, Van den Bossche P, Coosemans Th, Van Mierlo J. Electrical double-layer capacitors in hybrid topologies – assessment and evaluation of their performance. Energies 2012;5:4533–68.
[38] Amine K, Chen CH, Liu J, Hammond M, Jansen A, Dees D. Factors responsible for impedance rise in high power lithium ion batteries. J Power Sources 2011;97–98:684–7.
[39] Vetter J, Novak P, Wagner MR, Veit C, Möller KC, Besenhard JO, et al. Ageing mechanisms in lithium-ion batteries. J Power Sources 2005;147:269–81.
[40] Broussely M, Biensan Ph, Bonhomme F, Blanchard Ph. Main aging mechanisms in Li ion batteries. J Power Sources 2005;146:90–6.
[41] Stamps AT, Holland CHE, White RE, Gatzke EP. Analysis of capacity fade in a lithium ion battery. J Power Sources 2005;150:229–39.
[42] Wright RB, Chrisophersen JP, Motloch CG, Belt JR, Ho CD, Battaglia VS, et al. Power fade and capacity fade resulting from cycle-life testing of Advanced Technology Program lithium-ion batteries. J Power Sources 2003;119–121:865–9.
[43] Wright RB, Motloch CG, Christophersen JP, Ho CD, Richardson RA, Bloom I, et al. Calendar and cycle-life study of advanced technology development program generation 1 lithium-ion batteries. J Power Sources 2002;110:445–70.
[44] Bloom I, Cole BW, Sohn JJ, Jones SA, Polzin EG, Battaglia VS, et al. An accelerated calendar and cycle life study of Li-ion cells. J Power Sources 2001;101:238–47.
[45] Ning G, Haran B, Popov BN. Capacity fade study of lithium-ion batteries cycled at high discharge rates. J Power Sources 2003;117:160–9.
[46] Wang J, Liu P, Hicks-Garner J, Sherman E, Soukiazian S, Verbrugge M, et al. Cycle-life model for graphite-LiFePO$_4$ cells. J Power Sources 2011;196:3942.
[47] Ecker M, Gerschler JB, Vogel J, Käbitz S, Hust F, Dechent P, et al. Analyzing calendar aging data towards a lifetime prediction model for lithium-ion batteries. In: Proceedings EVS 26; 2012, USA.
[48] Kassem M, Bernard J, Revel R, Pélissier S, Duclaud F, Delacourt C. Calendar aging of a graphite/LiFePO$_4$ cell. J Power Sources 2012;208:296–305.
[49] Amine K, Liu J, Belharouak I. High-temperature storage and cycling of C-LiFePO$_4$/graphite Li-ion cells. Electrochem Commun 2005;7:669–73.
[50] Song H, Cao Zh, Chen X, Lu H, Jia M, Zhang Zh, et al. Capacity fade of LiFePO$_4$/graphite cell at elevated temperature. J Solid State, Electrochem 2012.
[51] Thomas EV, Case HL, Doughty DH, Jungst RG. Accelerated power degradation of Li-ion cells. J Power Sources 2003;124:254–60.
[52] Omar N, Daowd M, Van den Bossche P, Hegazy O, Smekens J, Coosemans Th, et al. Rechargeable energy storage systems for plug-in hybrid electric vehicles – assessment of electrical characteristics. Energies 2012;5:2952–88.
[53] ISO 12405-2 Electrically propelled road vehicles – Test specification for lithium-ion traction battery packs and systems – Part 1: High-energy applications. <http://www.iso.org/iso/home/store/catalogue_ics/catalogue_ics_browse.htm?ICS1=43&ICS2=120>; 2013 [07.01.13].
[54] PEC website. <http://www.peccorp.com/SBT0550-tabs-glance.html>; 2012 [15.12.12].
[55] CTS website. <http://www.ctsbenelux.be/Page.asp?DocID=99987&langue=NL>; 2012 [15.12.12].
[56] Zhang Y, Wang Ch, Tang X. Cycling degradation of an automotive LiFePO$_4$ lithium-ion battery. J Power Sources 2011;196:1513–20.
[57] Ramadass P, Haran B, White R, Popov BN. Capacity fade of Sony 18650 cells cycled at elevated temperatures Part I – Cycling performance. J Power Sources 2002;112:606–13.
[58] Waag W, Käbitz S, Uwe Sauer D. Experimental investigation of the lithium-ion battery impedance characteristic at various conditions and aging states and its influence on the applications. J Appl Energy 2012;102:885–97.
[59] Jespersen JL, Tonnesen AE, Norregaard K, Overgaard L, Elefsen F. Capacity measurements of li-ion batteries using AC impedance spectroscopy. World Elect Vehicle J 2009;3.
[60] Nagpure SC, Bhushan B, Babu SS, Rizzoni G. Scanning spreading resistance characterization of aged li-ion batteries using atomic force microscopy. Scripta Mater 2009;60:933–6.
[61] Nagpure SC, Dinwiddie R, Babu SS, Rizzoni G, Bhushan B, Frech T. Thermal diffusivity study of aged li-ion batteries using flash method. J Power Sources 2010;195:872–6.
[62] Xuezhe W, Bing Zh, Wei X. Internal resistance identification in vehicle power lithium-ion battery and application in lifetime evaluation. international conference on measuring technology and mechatronics automation; 2009, China.
[63] Dubarry M, Liaw BY. Identify capacity fading mechanism in a commercial LiFePO$_4$ cell. J Power Sources 2005;147:260–81.
[64] Bai P, Cogswell DA, Bazant MZ. Suppression of phase separation in LiFePO$_4$ nanoparticles during battery discharge. Nano Lett 2011;11:4890–6.
[65] Peterson SB, Apt J, Whitacre JF. Lithium-ion battery cell degradation resulting from realistic vehicle and vehicle-to-grid utilization. J Power Sources 2010;195:2385–92.
[66] Rosenkranz Ch. Deep cycle batteries for plug-in hybrid application. In: Proceedings EVS 20; 2003, France.
[67] Sato N. Thermal behaviour or analysis of lithium-ion batteries for electric and hybrid vehicles. J Power Sources 2001;99:70–7.
[68] Schaltz E. Design of fuel cell hybrid electric vehicle drive system. PhD thesis, University of Aalborg; 2009, Denmark.
[69] Peukert W. Über die Abhänigkeit der Kapazität von der Entladestromstärke bei Bleiakkumulatoren. Elektrotechnische Zeitschrift 1897;27:287–8.
[70] Wang J, Liu P, Hicks-Garner J, Sherman E, Soukiazian S, Verbrugge M, et al. Cycle-life model for graphite-LiFePO$_4$ cells. J Power Sources 2011;196:3942–8.
[71] Anseán D, Viera JC, González M, Garcia VM, Blanco C, Corte H. Fast charge protocol evaluation of lithium iron phosphate batteries for electric vehicles. In: Proceedings European electric vehicle congress; 2012, Brussels.
[72] Li J, Murphy E, Winnick J, Kohl PA. Studies on the cycle life of commercial lithium ion batteries during rapid charge-discharge cycling. J Power Sources 2001;102:294–301.
[73] Bishop J, Axon C, Bonilla D, Tran M, Banister D, McCulloch M. Evaluating the impact of V2G services on the degradation of batteries in PHEV and EV. Appl Energy 2013;111:206–18.
[74] Markovsky B, Rodkin A, Cohen YS, Palchik O, Levi E, Aurbach D, et al. The study of capacity fading processes of Li-ion batteries: major factors that play a role. J Power Sources 2003;119–121:504–10.
[75] Dubarry M, Liaw BY, Chen MS, Chyan SS, Han KC, Sie WT, et al. Identifying battery aging mechanisms in large format Liion cells. J Power Sources 2011;196:3420–5.
[76] Szczepanek A, Botsford C. Electric vehicle infrastructure development: An enabler for electric vehicle adoption. In: Proceedings EVS 24; 2009, Norway.
[77] Van den Bossche P. Electric and hybrid vehicles. Elsevier, 2010; p. 2517–44 [chapter].